Hindawi
Structural Control and Health Monitoring
Volume 2023, Article ID 6705090, 22 pages
https://doi.org/10.1155/2023/6705090

Research Article

A Multistation 3D Point Cloud Automated Global Registration and Accurate Positioning Method for Railway Tunnels

Jijun Wang,[1,2,3] **Xiao Wei**,[1,2,3] **Weidong Wang**,[1,2,3] **Jin Wang**,[1,2,3] **Jun Peng**,[1,2,3] **Sicheng Wang**,[1,2,3] **Qasim Zaheer**,[1,2,3] **Jia You**,[4] **Jianping Xiong**,[5] **and Shi Qiu**[1,2,3]

[1]*School of Civil Engineering, Central South University, Changsha 410075, China*
[2]*MOE Key Laboratory of Engineering Structures of Heavy-haul Railway, Central South University, Changsha 410075, China*
[3]*Center for Railway Infrastructure Smart Monitoring and Management, Central South University, Changsha 410075, China*
[4]*China Academy of Railway Sciences, Beijing 100000, China*
[5]*Guangxi Transportation Science and Technology Group Co. Ltd., Nanning 530006, China*

Correspondence should be addressed to Shi Qiu; sheldon.qiu@csu.edu.cn

Received 27 March 2023; Revised 23 September 2023; Accepted 28 September 2023; Published 16 October 2023

Academic Editor: Hoon Sohn

Terrestrial laser scanning (TLS) technology has the advantages of wide range, high efficiency, and low cost in spatial information collection, so it is widely used in infrastructure monitoring and measurement. During TLS application, the registration and positioning of the point cloud have a direct impact on the quality of the data and the validity of the results. The linear distribution of the tunnel structure and the lack of significant features present challenges in the registration and positioning of 3D point clouds in railway tunnels. The commonly used registration methods are difficult to achieve high registration accuracy and are prone to propagation errors, which reduce the accuracy and effectiveness of results. To achieve accurate registration and positioning of multistation clouds in railway tunnels, we propose a coordinate-based global registration method. To determine the coordinates of scan points in the reference coordinate system and the direction of the reference coordinate system, a few fixed control points are used during the data collection stage. Consequently, each station cloud can be precisely positioned and automatically registered in the reference coordinate system without accumulating or propagating errors. In addition, the coordinate-based registration method eliminates the introduction of errors due to artificial target setting and feature point extraction, as well as the problem of accurately positioning the entire point cloud in the reference coordinate system, thereby enhancing the accuracy, efficiency, and automation levels of cloud registration. The experiment demonstrates that the coordinate-based global registration method is robust and applicable in complex scenes, and it is suitable for the accurate positioning and registration of multistation clouds in linear and curved railway tunnels. The coordinate-based registration method reduces the amount of error in the global registration link by 65% when compared to the point-based registration method, and the point cloud accuracy has reached fine registration, ensuring that fine-grained inverse modeling of the tunnel structure can be performed.

1. Introduction

Geometry detection and monitoring of railway tunnels is an imperative task throughout their life cycle. This includes monitoring rock convergence during the construction phase and geometry detection during the operation phase. This directly affects the safe construction and stable operation of the tunnel [1]. The traditional measurement method is to use the total station or theodolite to continuously measure the fixed measurement points, analyze the measurement information at different times, and then realize the effective identification and monitoring of the geometric evolution process [1, 2]. The traditional measurement method is inefficient, time-consuming, and labor-intensive. In addition, due to the limited time for inspection and maintenance, the surveyor can only obtain the spatial information of a small

number of measurement points, which makes it difficult to realize the comprehensive monitoring of the real geometric position and safety status of railway tunnels [1].

In recent years, with the gradual maturity of terrestrial laser scanning (TLS) technology, TLS provides novel ideas and methods for geometric position detection and monitoring during the whole life cycle of the tunnel [2]. There are several applications of TLS in the tunnel field, including over-excavation and under-excavation detection, detecting the displacement of the initial support and calculating its thickness during construction, detecting secondary lining thickness during construction, and monitoring structural deformation throughout operation [3–6]. TLS can obtain spatial data of tunnels in different historical periods more conveniently, efficiently, and comprehensively than traditional monitoring and measurement methods. The use of this method greatly facilitates the extraction of key spatial information and the analysis of the structural status of tunnels [7].

Tunnel monitoring and measurement require a high degree of accuracy. Usually, when the deformation of a tunnel exceeds the limit by a few centimeters, it can have a serious impact on its safety and stability [1]. The point cloud acquired by a single TLS station has millimeter-level accuracy, which is sufficient for tunnel monitoring and measurement. However, the registration and positioning process of multiple stations will inevitably introduce errors. This is especially true when the scanning target is a linear strip structure. The small initial registration and positioning errors will be greatly amplified with the increase in the testing distance and the number of stations, resulting in propagation errors [1, 8, 9]. Pejić used a point-based registration method for the registration of the tunnel with a length of 1260 m. Due to the propagation and cumulative effect of the registration error between the stations, the final registration error of the global point cloud reaches 1 m [8]. Tunnel structures typically experience propagation errors that are much higher than the monitoring and measurement accuracy required, and more importantly, fine registration methods such as iterative closest point (ICP) and random sample consensus (RANSAC) cannot effectively correct propagation errors [1, 10]. Control of propagation errors can only be achieved by improving the global registration accuracy of the point cloud and reducing the initial error.

Currently, the most widely used global registration methods can be divided into three categories: point-based registration methods, line-based registration methods, and surface-based registration methods [11, 12]. Among them, point-based registration methods are the most widely adopted global registration methods [13]. This method extracts the common feature points of different station clouds manually or automatically. It uses common feature points as point connections to achieve registration of multiple station clouds [11]. The extraction of feature points is the key to this type of registration method. Point cloud registration is directly affected by the accuracy of its extraction. Early feature extraction algorithms include point feature histograms [14], spin images of points [15], or scale-invariant feature transform [16], but the above methods suffer from low noise sensitivity, low robustness, low computational efficiency, and difficulty in achieving high accuracy [17, 18]. Subsequently, Hänsch et al. [19, 20] proposed a series of registration methods based on area features, which are based on the geometric topological information of the area where the feature points are located to achieve feature point extraction and multisurvey site cloud registration, effectively improving global registration accuracy. The 4-point congruent sets (4PCS) and super four-point congruent set (S4PCS) algorithms, developed by Aiger et al. [21, 22] which use coplanar four points as their bases, have been developed, improving the global registration process' ability to adapt to noise and outliers, as well as improving global point cloud accuracy. However, sufficient overlap was required between the clouds at each survey site as part of the method. In addition, point-based registration methods all require the scan target to have a distinct feature structure, such as building vertices and corners [11].

Line-based registration methods include line feature translation [23], Laplacian matrix decomposition [24], and point cloud segmentation based on TIN [25]. Lines have a stronger geometric topology and constraint than points, which results in a higher level of registration accuracy [26, 27]. It is commonly used in large-scale 3D point cloud scenes [11] such as urban roads and large buildings. Compared to points and lines, surfaces have richer geometric features, and surface-based registration methods are less affected by noise and have better registration accuracy. Least squares [28], conjugate surface features [29], and principal component analysis methods are commonly employed for surface extraction, and the extracted surfaces are mainly ground, roof, and building facades. Although line-based registration methods and surface-based registration methods have higher registration accuracy, the 3D point cloud scene used for registration must contain a large number of feature structures with explicit geometric information; otherwise, registration accuracy is difficult to guarantee [30]. Registration is an indispensable process in the preprocessing of 3D point cloud data. The registration process can be divided into two stages: coarse registration and fine registration. In the field of railway tunnel engineering, global registration is generally used to refer to coarse registration [8, 31–34]. Global registration involves the stitching of multiple clouds together, which provides a reliable base point cloud for fine registration. Fine registration optimizes the global point cloud in detail. A global point cloud with high accuracy can, on the one hand, effectively reduce the computation of fine registration and avoid falling into a local optimum. In addition, it can solve some problems that cannot be effectively solved by the fine-registration process. These problems include propagation errors [22]. Global registration is the basis of the whole registration work, and the accuracy of global registration is the key to the whole registration process. The existing global registration methods have made significant progress in terms of robustness, computational efficiency, and registration accuracy. However, applicability for railway tunnels is still low, and they are difficult to achieve high accuracy and are highly prone to propagation errors. Accurate global

registration and positioning of multisurvey site clouds in railway tunnels remain a problem that has not yet been solved.

This paper proposes a method for precisely registering and positioning a point cloud within a railway tunnel. Using a limited number of existing control points, this method accurately locates the coordinate information and reference system direction of the scanned points in the reference coordinate system. During the data acquisition phase, point clouds are precisely located within the reference coordinate system. This allows automatic and accurate registration of point clouds within the reference coordinate system. As a result of the method, error introduction processes such as artificial target setting and feature point extraction are avoided for the global registration of multistation clouds in railway tunnels, the initial registration accuracy and propagation error control are improved, and the problem of accurate positioning of the global point cloud in the reference coordinate system is resolved. In comparison with the point-based global registration method, the error of the coordinate-based method has been reduced by 65%, and the accuracy of global point cloud registration has reached that of fine registration.

2. Problem Statement and Research Objectives

According to the technical principle of TLS, the distance from the scanning point to the target can be calculated by calculating the time difference between the laser doing a roundtrip flight between the scanning point and the target. Combining the laser emission angle with the three-dimensional coordinates of the target under the relative coordinate system allows us to collect spatial information about the scanned target. TLS employs fixed stations for 3D scanning, and individual stations often cannot acquire comprehensive spatial information for large-scale scenes, such as railway tunnels. Multiple stations must be set up to scan different areas; subsequently, the station clouds are sequentially aligned and positioned in order to obtain a global point cloud containing comprehensive 3D information about railway tunnels; as a result of the global point cloud, geometric information and state analysis of railway tunnels can be conducted. The technical flow of TLS for monitoring and measurement in railway tunnels is shown in Figure 1.

Global registration is a key step in the preprocessing of multistation clouds, and this step directly affects the accuracy of the global point cloud and the validity of the detection results. Currently, three types of global registration methods are commonly employed: point-based registration, line-based registration, and surface-based registration [12]. Due to their extremely symmetrical cross-sections, railway tunnels lack distinctive feature structures. Existing global registration methods do not apply to railway tunnels under the condition that manual targets are not employed [30]. A method based on artificially constructed feature points has been widely used for the global registration of point clouds in railway tunnels [3, 31, 35, 36]. Researchers generally set up at least three targets in the common scanning area of neighboring stations and use manual or automated methods to extract common feature points on the targets. One of the point clouds is set as the reference point cloud, and the coordinate information of the common feature points is used to calculate the translation and rotation matrices for the registration of the target point cloud to the reference point cloud. The other station clouds are sequentially aligned to the reference point cloud by means of rigid transformation to realize the global registration of multistation clouds. The station clouds are stitched together into a whole by relying on the above feature points in order to facilitate global registration. Artificially constructed feature points are placed among stations through targets in order to achieve global registration. As points contain less geometric and topological information than lines and surfaces, it is difficult to achieve high global registration accuracy with point-based registration methods compared to other global registration methods [27]. In addition, the above global registration method has the following three shortcomings: (1) the tunnel site environment is complex, with pedestrians, vehicle vibrations, and wind causing displacement of the target, resulting in the feature points used for registration at each station not being the same point in the reference coordinate system [4]; (2) it is difficult to accurately extract multiple common feature points from a large number of point clouds [25]; (3) it is not possible to accurately position the overall point cloud in the reference coordinate system, and secondary adjustments are required [4]. This will lead to errors in global registration and positioning, and more importantly, railway tunnels are linearly distributed. As the sampling range and the number of scanning stations increase, the initial registration errors will gradually accumulate and amplify. These errors will form propagation errors, which greatly reduce the accuracy and availability of the global point cloud. In general, when TLS is used for monitoring and measuring railway tunnels, the accurate registration and positioning of multistation clouds is still a problem that has not been solved, which to a certain extent also restricts the large-scale application of TLS technology in the railway field.

In this paper, we propose a coordinate-based global registration method for railway tunnels. It has been proved experimentally that the coordinate-based global registration method has higher registration and localization accuracy than the point-based global registration method, which is more suitable for accurate global registration and localization in railway tunnels. This method avoids the error introduction process associated with target setting and feature extraction. It adopts the strategy of aligning each cloud station to the reference coordinate system independently. This means that there is no cumulative effect in the registration process of each station cloud and has higher registration accuracy.

3. Methodology

3.1. Principle of Coordinate-Based Global Registration Technology. The key to the implementation of the coordinate-based registration method is to precisely locate

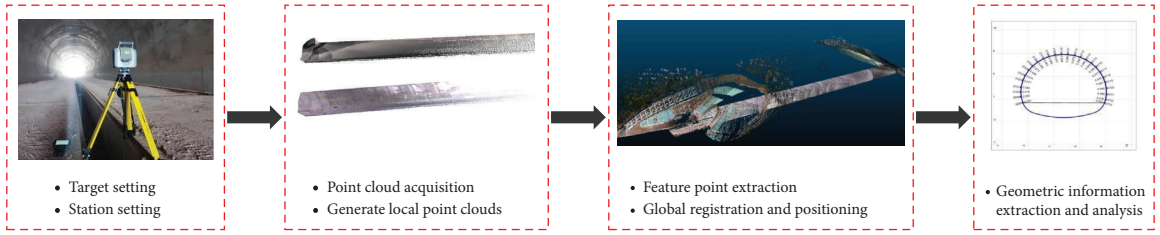

Figure 1: TLS for railway tunnel monitoring and measurement process.

the coordinates of the laser scanner under the reference coordinate system as well as the due east, due north, and vertical directions of the reference coordinate system before data acquisition, and the specific implementation steps of the method are as follows.

(1) *Precise Positioning of Control Points*. The CPIII coordinate network is used in China in the construction of numerous large infrastructures. It is used for finding site coordinates and assessing construction quality. Multiple control points with permanent coordinate information are set up for construction guidance and active monitoring and measurement during the construction period for tunnels, bridges, and other critical structures. In this paper, two control points at the tunnel entrance are selected as the basic control points to accurately locate the precise coordinate information of the scanned points in the reference coordinate system and identify the specific direction of the reference coordinate system, with the control point numbers: #C1 (x_1, y_1, z_1) and #C1 (x_2, y_2, z_3).

(2) *Key Geometric Information Extraction*. A reflective prism was placed on the control point with explicit coordinate information, as shown in Figure 2, and the rod heights l_1 and l_2 were recorded, and then the coordinates of the prism measurement points were $(x_1, y_1, z_1 + l_1)$ and $(x_2, y_2, z_3 + l_2)$; subsequently, we set up scanning stations and leveled the scanner. Finally, we used scanning to measure the distance and angle of points #C1 and #C2 and obtained the distance and vertical angle between the measurement points and the control points. In addition, before the test starts, it must be clear that each station is located east or west of the control point. The key geometric information is summarized as shown in Table 1.

(3) *Scanning Point Positioning and Reference Coordinate System Orientation*. Using the key geometric information obtained in step 2, the coordinate information of the scan point under the reference coordinate system is accurately calculated. Based on this, the due east, due north, and vertical directions under the reference coordinate system are precisely located.

In step 2, the position relationship between the collector scan point and the prism measurement point in the xy plane projection is shown in Figure 3. The scanning point #S_n and the measurement points #C1 and #C2 satisfy the following equations:

$$\left(x_1 - x_{S_n}\right)^2 + \left(y_1 - y_{S_n}\right)^2 = l_1^2, \tag{1}$$

$$\left(x_1 - x_{S_n}\right)^2 + \left(y_1 - y_{S_n}\right)^2 = l_1^2, \tag{2}$$

$$l_1 = L_1 \cos \alpha_1, \tag{3}$$

$$l_2 = L_2 \cos \alpha_2, \tag{4}$$

where x_1 and y_1 are the east and north coordinates of point #C1; x_2 and y_2 are the east and north coordinates of #C2; x_{S_n} and y_{S_n} are the east and north coordinates of #S_n, respectively; L_1 and l_1 are the linear distance between #S_n and #C1 and the projection distance in the xy plane; L_2 and l_2 is the linear distance between the #S_n point and the #C2 point and the projection distance in the xy plane; α_1 is the vertical angle between the #S_n point and the #C1 point; and α_2 is the vertical angle between the #S_n point and the #C2 point.

Equation (3) is solved in conjunction with equation (4) to obtain two solutions about the coordinates of the #$S_n$point: $(x_{s_{n1}}, y_{s_{n1}})$ and $(x_{s_{n2}}, y_{s_{n2}})$, and the two points are symmetric about the line where the #C1 point and #C2 point are located, and the calculation formula is shown in equation (1) ~ equation (2).

Table 1: Relevant parameters.

Parameter category	Parameter description
α_1	$S_n - C_1$ ray vertical angle
α_2	$S_n - C_2$ ray vertical angle
L_1	Distance between point C_1 and point S_n
L_2	Distance between point C_2 and point S_n

(a) (b)

Figure 2: Schematic diagram of data acquisition. (a) Laser scanner placement schematic. (b) Prismatic and railway tunnel control points.

$$\begin{cases} x_{s_{n1}} = a - \dfrac{(L_1 \sin\alpha_1)^2 - (a - x_1)^2 - (b - y_1)^2}{\sqrt{1 + k^2}}, \\ y_{s_{n1}} = b + k(x_{sn1} - a), \end{cases}$$

$$\begin{cases} x_{s_{n2}} = a + \dfrac{(L_1 \sin\alpha_1)^2 - (a - x_1)^2 - (b - y_1)^2}{\sqrt{1 + k^2}}, \\ y_{s_{n2}} = b + k(x_{sn2} - a), \end{cases} \tag{5}$$

$$a = x_1 + \frac{\left[(L_1 \sin\alpha_1)^2 - (L_2 \sin\alpha_2)^2 + (x_2 - x_1)^2 + (y_2 - y_1)^2\right] \cdot (x_2 - x_1)}{2\left[(x_2 - x_1)^2 + (y_2 - y_1)^2\right]},$$

$$b = y_1 + \frac{\left[(L_1 \sin\alpha_1)^2 - (L_2 \sin\alpha_2)^2 + (x_2 - x_1)^2 + (y_2 - y_1)^2\right] \cdot (y_2 - y_1)}{2\left[(x_2 - x_1)^2 + (y_2 - y_1)^2\right]},$$

$$k = \frac{x_2 - x_1}{y_1 - y_2}.$$

Since $\#S_n$, $\#C1$, and $\#C2$ are not in a straight line, $x_{s_{n1}} \neq x_{s_{n2}}$. When the scan point is located east of the reference point, then x_{s_n} takes the maximum of $x_{s_{n1}}$ and $x_{s_{n2}}$ and the corresponding y_{s_n}. When the scan point is located west of the reference point, then x_{s_n} takes the minimum of $x_{s_{n1}}$ and $x_{s_{n2}}$ and the corresponding y_{s_n}.

For the elevation of the scanned point S_n, the calculation is performed by the following equation:

$$z_{s_n} = \frac{(z_1 + l_1 - L_1 \cos\alpha_1) + (z_2 + l_2 - L_2 \cos\alpha_2)}{2}, \tag{6}$$

where z_{s_n} is the elevation of the scanning point $\#S_n$ in the reference coordinate system, z_1 and z_2 are the elevations of points $\#C1$ and $\#C2$, respectively, l_1 and l_2 are the prism heights of points $\#C1$ and $\#C2$, respectively, α_1 is the vertical angle between point $\#S_n$ and point $\#C1$, and α_2 is the vertical angle between point $\#S_n$ and point $\#C2$. The exact

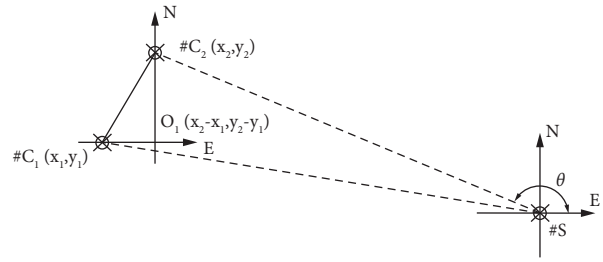

Figure 3: Principle of the coordinate-based registration method.

coordinates of the scanned points of each station in the reference coordinate system can be obtained by the above process, which is noted as $\#S_n(x_{s_n}, y_{s_n}, z_{s_n})$.

As each station was manually leveled before data collection started, the vertical direction under the reference coordinate system was already established. In addition, the due east and due north directions of the reference coordinate system were determined. The vertical direction has been determined under the premise that the due east and due north directions are separated by 90 degrees. The essence of the orientation work is to determine the due east direction. Since the coordinates of $\#S_n$, $\#C1$, and $\#C2$ are known, in the plane where xy is located, the vector $\overrightarrow{S_nC2}$ is $[x_2 - x_{s_n}, y_2 - y_{s_n}]$, and the unit vector of the due east direction is [1, 0], which is noted as $\overrightarrow{e}$. The angle between the above two vectors according to the cosine theorem is calculated.

$$\cos\theta = \frac{\left[\overrightarrow{S_nC1}, \overrightarrow{e}\right]}{\left\|\overrightarrow{S_nC1}\right\| \|\overrightarrow{e}\|},$$
$$\theta = \arccos\left(\frac{x_2 - x_n}{\sqrt{\left(x_2 - x_{s_n}\right)^2 + \left(y_2 - y_{s_n}\right)^2} \cdot 1}\right). \tag{7}$$

When $y_2 - y_{s_n} > 0$, $\theta_{s_n} = \theta$. When $y_2 - y_{s_n} < 0$, $\theta_{s_n} = 2\pi - \theta$.

The above process determines the coordinates of each station's scanning point in the reference coordinate system and the angle between the $S_n - C_2$ and the due east direction. In the process of point cloud data acquisition, first of all, the acquisition instrument is strictly leveled, and the direction of the Z axis of the reference coordinate system is clearly defined, i.e., the vertical direction of the reference coordinate system. Then, the horizontal direction of the scanner is calibrated using θ_{s_n}.

The positioning and registration of each measurement site cloud in the reference coordinate system are done by rigid transformation, the principle of which is shown in the following equation:

$$P_t = R \cdot P_s + T, \tag{8}$$

where P_s is the set of point clouds in the coordinate system, P_t is the corresponding set of point clouds in the reference coordinate system, R is the rotation matrix, and T is the translation matrix.

$$\begin{bmatrix} X_i \\ Y_i \\ Z_i \end{bmatrix} = R \cdot \begin{bmatrix} x_i \\ y_i \\ z_i \end{bmatrix} + T, \tag{9}$$

where (x_i, y_i, z_i) is a specific individual point in P_s and (X_i, Y_i, Z_i) is the corresponding point in the reference coordinate system.

In the point cloud data acquisition process, the scanned points are the initial coordinates of (0, 0, 0) under the local coordinate system. Since the coordinates of the scanned points of each station are known under the reference coordinates, the translation matrix can be derived as $(x_{S_n}, y_{S_n}, z_{S_n})^T$. Since the scanner is strictly leveled, the local coordinate system Z axis is parallel to the reference coordinate system Z axis, and the only thing to be considered is the rotation of the xy plane, and the angle between the local coordinate system and the reference coordinate system due east is known to be θ_{s_n}, so the rotation matrix R can be found.

$$R = \begin{bmatrix} \cos\theta_{sn} & -\sin\theta_{sn} & 0 \\ \sin\theta_{sn} & \cos\theta_{sn} & 0 \\ 0 & 0 & 0 \end{bmatrix}. \tag{10}$$

Through the above process, the translation and rotation matrices for the positioning and registration of each station cloud to the reference coordinate system are obtained before the data collection of each station, and the coordinates and directions of each station are calibrated. In this way, the coordinate information of the point cloud acquired by each station is the real coordinate information of the measurement target in the reference coordinate system, and the accurate positioning and registration of each station cloud in the reference coordinate system are completed during the data acquisition process.

3.2. Technical Advantages of the Coordinate-Based Global Registration Method. Point-based registration is the most widely used global registration method for TLS applications in tunneling [3, 31, 35, 36]. Using targets between stations, distinct feature points are constructed, and feature points are used to connect different station clouds. Connecting the different station clouds is done through feature points. However, point-based registration methods are difficult to reach with high registration accuracy and are subject to propagation errors, severely reducing the accuracy and availability of global point clouds. Here are some of the main reasons for the above problems.

(i) In the data acquisition stage, external factors such as wind, pedestrian, or vehicle vibrations can cause displacement of the target due to the complex environment of the tunnel site. In addition, the scanning area of the target is not the same for each station. This is especially obvious when the station is far away from the target, resulting in a large distance between the point clouds. All of these factors can lead to the extraction of feature points that are not the same point in real space, which can cause initial registration errors.

(ii) In the feature point extraction stage, due to the limited geometric and topological information contained in the points, it is difficult to achieve a high level of accuracy for all types of feature point extraction algorithms, and errors are particularly noticeable. Although the accuracy of manually extracted feature points is significantly higher than that of automated methods, it is difficult and inefficient to accurately select at least three noncommon-linear common points in a large number of dense point clouds.

(iii) In the registration stage, each station cloud is aligned station by station along the longitudinal direction. The initial registration error will gradually accumulate as the distance and station data increase, forming a propagation error.

(iv) In the global point cloud positioning stage, secondary feature point extraction is required, a process that will further expand the error.

In this study, a coordinate-based global registration method for multistation clouds is proposed. The process shown in Figure 4 permits the precise positioning and automatic registration of the multisurvey site cloud of railway tunnels, with the specific steps described as follows. Compared with the point-based registration method, this method has the following advantages:

(i) *Higher Adaptability and Accuracy*. The coordinate-based registration method uses two control points to precisely locate the specific coordinates of the scan point in the reference coordinate system before data acquisition. Since the control point locations are constant and the positioning is done before data acquisition, the influence of external factors such as wind, pedestrian, or vehicle vibration on the data acquisition process is reduced.

(ii) *Avoid the Process of Target Setting and Feature Point Extraction*. The coordinate-based registration method precisely locates the coordinates of scanning points and the direction of the reference coordinate system, enabling the precise positioning and automatic registration of each station cloud in the reference coordinate system during the data acquisition stage. This method avoids the process of target setting and feature point extraction and improves the accuracy and automation of global registration while effectively controlling the introduced errors.

(iii) *Propagation Errors Are Controlled*. The point-based registration method adopts a station-by-station registration scheme, and the initial error of each station has a cumulative effect. In the coordinate-based registration method, each station is directly aligned with the reference coordinate system as the basis, and the registration process of each station is independent, so there is no cumulative effect of the initial registration error.

(iv) *Global Point Cloud without Secondary Positioning*. The coordinate-based registration method takes the actual construction coordinate system as the reference. First, each measurement point cloud under the reference coordinate system is located, and then the automatic registration of each measurement point cloud is performed. The positioning process of the global point cloud takes precedence over the registration process, so there is no need for secondary positioning. In addition, since the reference coordinate system is fixed, this also greatly facilitates the positioning and comparison of tunnel point cloud data in different historical periods under the same reference coordinate system.

4. Experiment

4.1. Data Acquisition. In this paper, a 220 m long railway tunnel in Guangxi, China, is selected for the experiment, as shown in Figure 5(a), and its cross-section information is shown in Figure 5(b). The concrete pouring for the second lining had been completed at the time of data collection, but the track system had not yet been laid. The second lining section is a standard arc with a radius of 6.41 m. To reduce the influence of system errors during data acquisition, this paper has developed the optimal station deployment plan under the condition of fully considering the data acquisition environment and the equipment's parameters. According to the requirements of different global registration methods for auxiliary equipment, the optimal layout plan of the target and prism is formulated.

In the development of a data acquisition program, sampling time, point cloud density, and point cloud accuracy play a key role. These factors directly affect the acquisition cost and quality of point clouds. Among them, the sampling duration is determined by the sampling mode and the number of stations. The point cloud density is controlled by the sampling distance, laser incidence angle, and station spacing. Also, the accuracy of the single station cloud is controlled by the sampling distance. The relationship between point cloud density, laser incidence angle, and sampling distance is shown in Figure 6. β is the angle between the incident laser and the normal direction of the measurement point, and the point spacing increases sharply

with the increase of the incidence angle when the vertical distance between the incident laser and the scanning plane remains unchanged.

All stations are located on the central axis of the railway tunnel. The laser scanning point from the tunnel vault and the distance between the two sides of the tunnel are 8.1 m and 6.3 m. The lowest value of point cloud density and accuracy for each section of the tunnel occurs at the top of the arch, point A in Figure 5. When the point cloud quality at point A meets the requirements, the point clouds in other areas also meet the requirements. The straight line that passes through point A along the tunnel's longitudinal axis is taken. This is the subject of the research, and the relationship between point spacing and laser incidence angle is as follows:

$$\Delta L_s = H \cdot (\tan(\beta + \Delta\beta) - \tan\beta), \tag{11}$$

$$L_s = H \cdot \tan\beta, \tag{12}$$

where L_s is the longitudinal sampling distance; β is the angle of incidence; H is the vertical distance between the scanning point and the vault; H is 8.1 m; and ΔL_s is the point spacing.

The Trimble SX10 laser scanner was used in this study. The laser scanner has a horizontal field of view of 360 degrees and a vertical field of view of 290 degrees. The sampling rate is 26,600 points/s, the range accuracy is 1 mm + 1.5 ppm, and the range is 600 m. The manufacturer of the Trimble SX10 did not explicitly give the angular resolution of different scanning modes but only the point spacing under different scanning modes when the forward range is 50 m, as shown in Table 2. We calculated the equivalent sampling angular resolution of the device in different sampling modes based on the following.

According to equations (11) and (12), we can calculate the relationship between point spacing and sampling distance, as well as the relationship between point spacing and incidence angle for various sampling modes, as illustrated in Figure 7.

Three factors need to be considered are as follows: (1) point cloud accuracy, to maximize the accuracy of the point cloud, we limit the sampling distance to 50 m; (2) point cloud density, considering the subsequent parameter extraction and analysis, to ensure that at least two points are generated per 10 cm or exactly four points per 100 cm^2 area; and (3) total sampling time is less, different sampling modes to meet the above three constraints of the acquisition program are presented in Table 3.

The paper selects option B based on the premise of fully considering the overall optimum of sampling time, point cloud density, and point cloud accuracy. The paper selects option B based on the premise of fully considering the overall optimum of sampling time, point cloud density, and point cloud accuracy. An effective sampling distance for one station is 30 m, the station spacing is 60 m, and five stations are set up. The layout and scanning area are shown in Figure 8. The station numbers are #$S1$, #$S2$, #$S3$, #$S4$, and #$S5$. The total sampling time was 150 minutes, and at least 6 points existed in the area of 100 cm^2 due to the superposition effect of point clouds between stations. The target arrangement is shown in Figure 8. A constant target group is placed 20 m from the entrance and exit, respectively, to reduce the error caused by target movement. Each target group consists of three noncoincident targets, and the target groups are numbered #$M1$ and #$M2$. When the point-based registration method is used for global registration, #$S1$, #$S2$, and #$S3$ stations are aligned with #$M1$ target groups and #$S3$, #$S4$, and #$S5$ stations are aligned with #$M2$ target groups.

4.2. Global Registration of 3D Point Clouds in Railway Tunnels. A 3D point cloud data acquisition scheme is proposed in this study taking into account the tunnel structure and parameters of the acquisition equipment. Despite ensuring the accuracy of the base point cloud of each station, a satisfactory balance is achieved in terms of point cloud density, sampling time, and error control. We propose a coordinate-based registration method in this paper in order to achieve accurate positioning and fast registration of multistation point cloud data in the reference coordinate system. Figure 9 illustrates the entire point cloud of the tunnel structure. Utilizing the macroscopic point cloud, we can effectively convey precise and accurate geometric information pertaining to the tunnel and slope. Moreover, we can determine the precise position of the overall point cloud in the reference coordinates. There is a uniform and smooth distribution of points at the fine level, which allows us to discern the geometric features of the tunnel's second lining surface. Furthermore, this method facilitates the comparison and analysis of tunnel structures throughout their entire life cycle. The point clouds of different historical periods are precisely positioned in the same reference coordinate system without the need for later adjustment of the coordinate system. As a result, continuous monitoring of the geometry of the railway tunnel in time, as well as identification of the state of service, is greatly facilitated.

4.3. 3D Point Cloud Inverse Reconstruction of a Railway Tunnel. To verify whether the global point cloud obtained by the coordinate-based registration method has high accuracy, this paper tries to inverse model the global point cloud of the railway tunnel to visually judge the accuracy of the base point cloud from the model perspective.

The internal environment of the unfinished tunnel structure is complex, with a large number of construction materials stored and workers and construction vehicles passing through the scanning area. This can lead to a large number of noise points and anomalies in the overall point cloud. In the process of 3D point cloud reconstruction, first, a large number of external point clouds such as slopes and trees outside the tunnel are eliminated. In contrast, dense anomalous point clouds inside the tunnel are removed at each station. This process is completed in the Trimble Business Center (TBC) software. Then, a segmentation method based on region growth is used to segment the second liner and bottom plate region data to facilitate subsequent accuracy analysis. Finally, this paper uses the

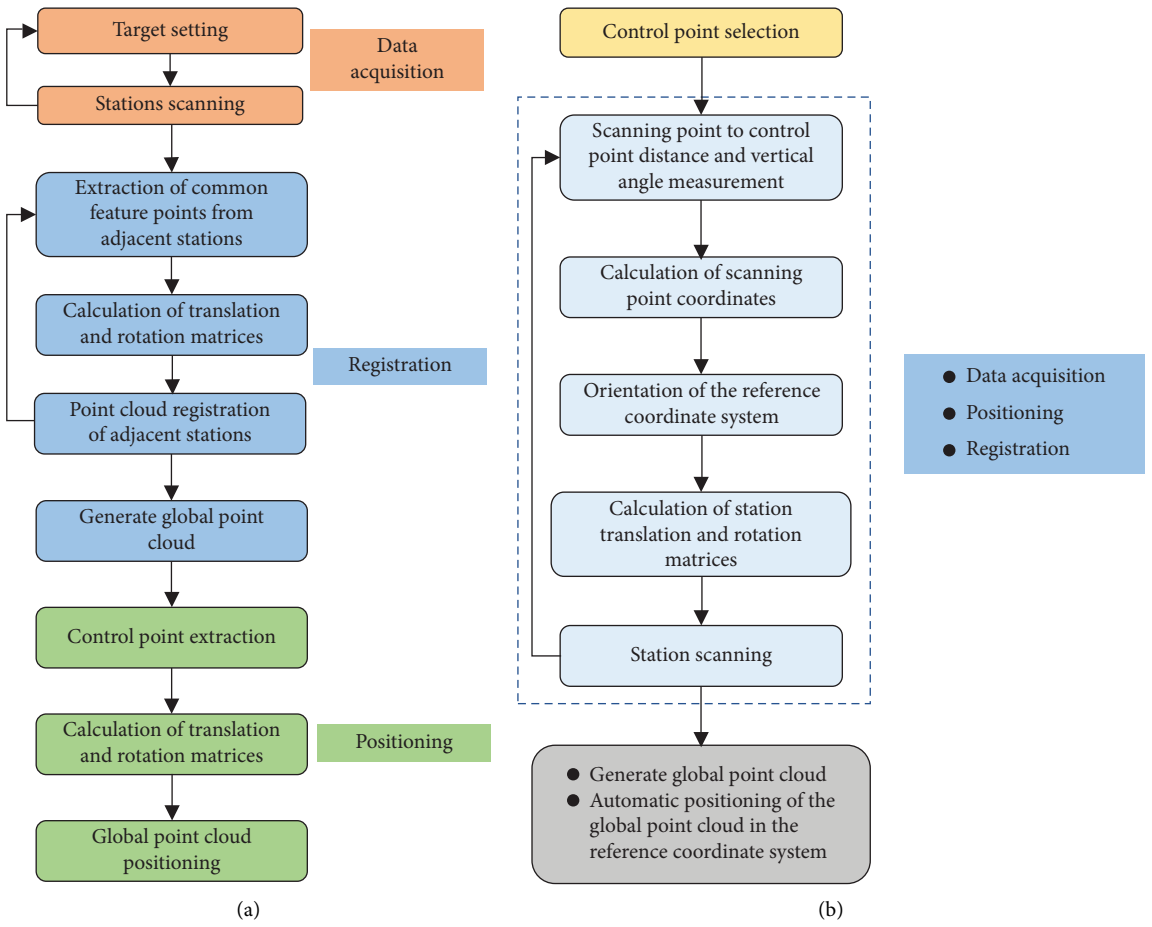

Figure 4: Process comparison of global registration methods. (a) Point-based global registration method. (b) Coordinate-based global registration method.

(a) (b)

Figure 5: (a) Test tunnel site. (b) Tunnel cross-section.

greedy triangular surface reconstruction method to inverse model the tunnel structure. The segmentation and modeling of the point cloud are being done in the Point Cloud Library (PCL) environment. The inverse model of the railway tunnel is shown in Figure 10.

At a macrolevel, the model clearly depicts the tunnel's main structure, such as the second lining and open hole, with a complete and smooth surface. The model provides a fine representation of defects in tunnel construction and the impressions of trolley grouting at the fine level. The point

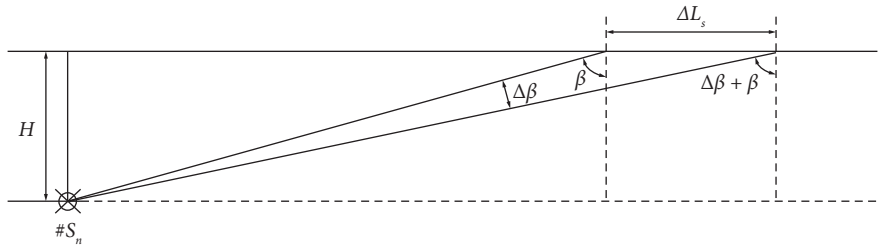

Figure 6: Point spacing calculation diagram.

Table 2: Information about different scanning modes.

Scan mode	Rough	Standard	Precision	Precision+
Point spacing (mm)	50	25	12.5	6.25
Number of scans	1	4	16	64
Number of horizontal scans	1	2	4	8
Angular resolution (degrees)	3.4	1.7	0.85	0.425
Scanning time (minutes)	12	30	200	800

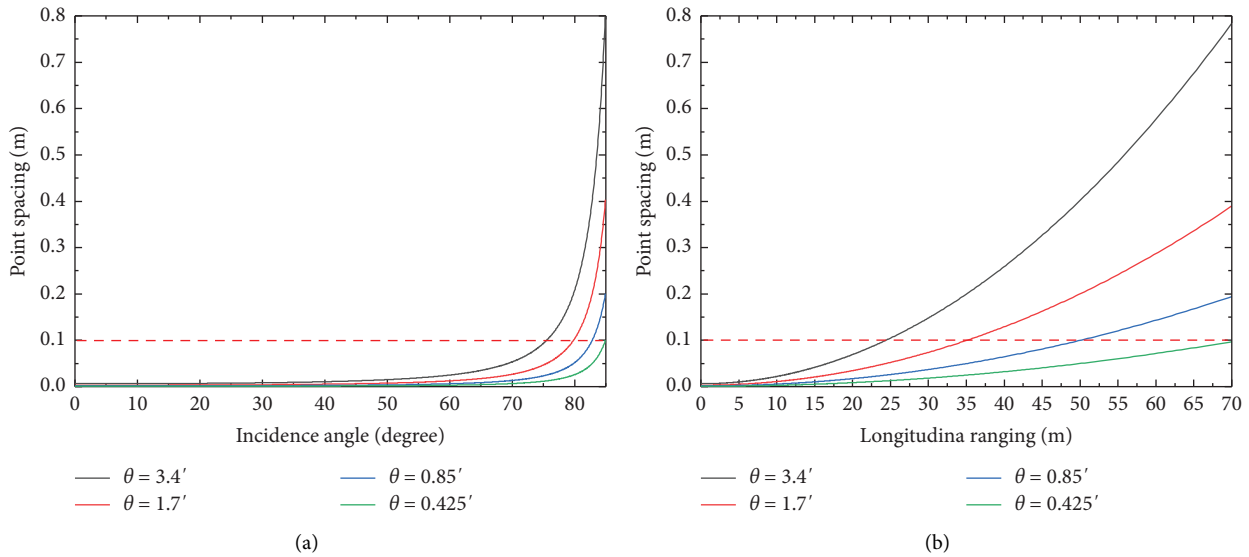

Figure 7: Point spacing distribution pattern. (a) The relationship between point cloud spacing and laser incidence angle. (b) The relationship between point cloud spacing and sampling distance.

Table 3: Different sampling mode stations and time duration.

Acquisition solutions	A	B	C	D
Sampling level	Rough	Standard	Precision	Precision+
The longitudinal distance of 10 cm distance between points	24	35	50	70
Angle of incidence	75	80	82.8	85
Number of measuring stations	7	5	3	3
Total sampling time (minutes)	94	150	600	2400

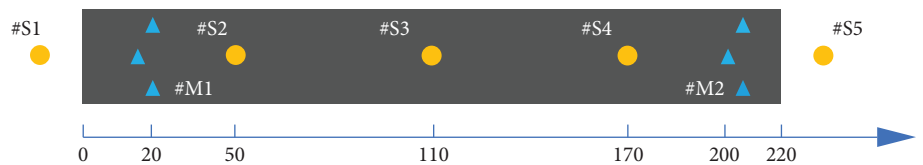

Figure 8: Schematic diagram of target and station arrangement.

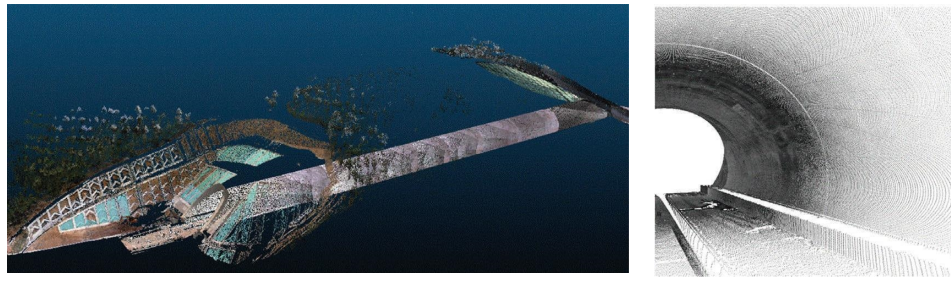

(a) (b)

Figure 9: (a) Railway tunnel global point cloud. (b) Point cloud of railway tunnel fine view.

cloud generated by the data acquisition and registration method proposed in this paper has excellent accuracy. It meets the requirements for accurate inverse modeling of the tunnel structure.

4.4. Registration Accuracy Comparison Experiments. As far as registration accuracy is concerned, the following experiments are designed to explore the improvement effect of coordinate-based registration over point-based registration. To evaluate the accuracy of point cloud registration, the offset distance between the overall point cloud and the standard model of the acquisition target is calculated and used [1]. There are two types of offset distances: point-to-point offset distance and point-to-surface offset distance [1]. Due to the absence of an obvious characteristic structure of the tunnel's second lining surface, it is difficult to accurately identify the corresponding points of the point cloud on the second lining structure, and as a result of the above reasons, this paper selects an offset distance between the point and the standard second lining surface as the registration accuracy evaluation index. It is not practical to use a total station to obtain accurate geometric information of the entire second lining surface in the selection of the ground truth. In this study, it is assumed that the tunnel's second lining surface fully meets the design requirements. This surface is selected as the ground truth for the calculation of point cloud offset distance. The measurement object in this study is a linear tunnel with zero tunnel slope and a circular lining section with a radius of 6.41 meters. Based on the coordinate-based registration method, the overall point cloud data have been positioned in the reference coordinate system and combined with the initial tunnel design files, so that the researcher can easily adjust the coordinates of the point cloud data. This paper adjusts the straight line at the center of the tunnel section to the values of $x = 0$ and $z = 0$. By using the above settings, we were able to easily compare the degree of fit between the point cloud data and the standard model section. A tunnel's second lining structure is a circular arc, and it follows the longitudinal direction of any section, satisfying the following equation:

$$x^2 + z^2 = R^2, \tag{13}$$

where x and z are the coordinate values of each point of the second lining section along the x and z axis directions in the relative coordinate system, and R is 6.41 m. The offset distance between the coordinate-adjusted overall point cloud and the standard second lining surface is calculated by the following equation:

$$\Delta l = \sqrt{x_i^2 + z_i^2} - R, \tag{14}$$

where x_i and z_i are the coordinate values of each point along the X and Z directions in the relative coordinate system. R is 6.41 m, and Δl is the offset of each point from the standard surface. In this paper, the average of the algebraic deviations (ΔR), the mean absolute error (MAE), and the root mean square error (RMSE) of the overall point cloud offset from the standard model are selected as the analysis indexes. The calculation formula for each index is as follows:

$$\begin{aligned} \Delta R &= \frac{1}{n}\sum_{i=1}^{n}\left(\sqrt{x_i^2 + z_i^2} - R\right), \\ \mathrm{MAE} &= \frac{1}{n}\sum_{i=1}^{n}\left|\sqrt{x_i^2 + z_i^2} - R\right|, \\ \mathrm{RMSE} &= \sum_{i=1}^{n}\sqrt{\frac{1}{n}\left(\sqrt{x_i^2 + z_i^2} - R\right)^2}. \end{aligned} \tag{15}$$

This paper conducts a comparative analysis of two stages, global registration and fine registration, to determine the improvement effect of the coordinate-based registration method over the point-based registration method in terms of registration accuracy. In the global registration stage, we use the coordinate-based registration method and the point-based registration method to register the point clouds of the five stations, respectively. Among them, the specific implementation process of the point-based registration method is as follows: first, two target groups, #M1 and #M2, are set up in the data acquisition phase, in which the #M1 target group is shared by the #S1, #S2, and #S3 stations, and the #M1 target group is shared by the #S3, #S4, and #S4 stations, as shown in Figure 8. Then, we use a manual approach to extract the feature points of

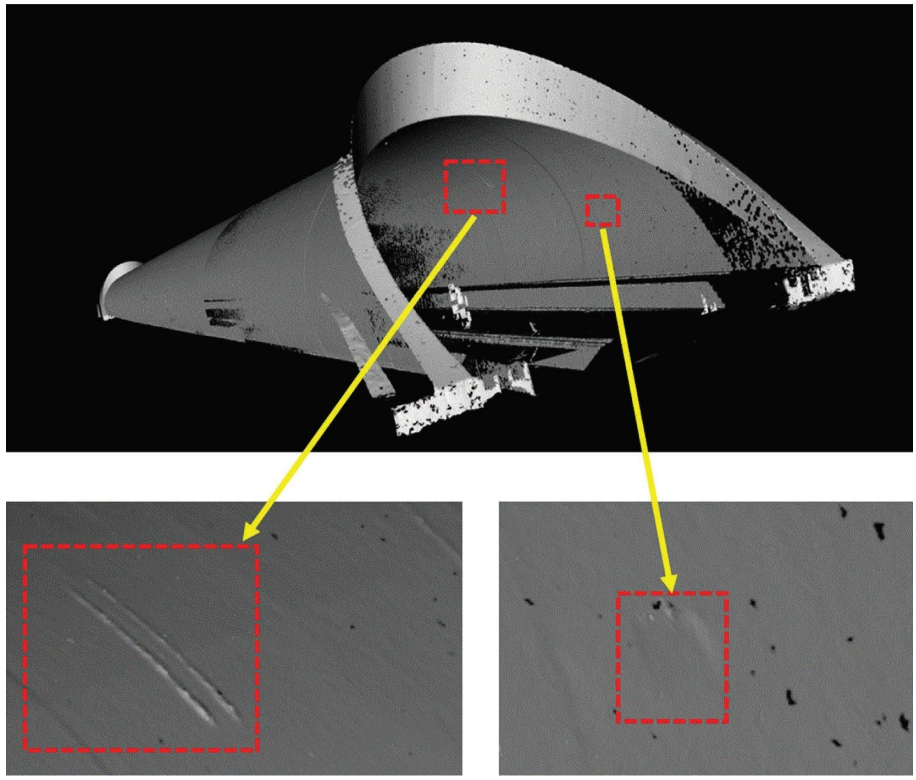

Figure 10: Tunnel inverse model.

the shared target group and use the coordinate information of the feature points to calculate the translation and rotation matrices. Finally, we set the coordinate system of #S1 as the reference coordinate system and use the rigid transformation to align the other station clouds in turn, calculated as shown in equation (9). It is worth noting that we have positioned the #S1 station cloud in the reference coordinate system before the registration, and since all the other station clouds use the #S1 station cloud as a reference, this means that the global point cloud will eventually be able to achieve the positioning to the reference coordinate system as well. In the fine-registration stage, two sets of global point clouds are fine registered using ICP algorithms, and the accuracy of the two sets of point clouds after fine registration is compared.

As shown in Figure 11, the coordinate-based registration method is significantly more accurate than the point-based registration method at the global registration stage. The mean values of the global point cloud offset obtained by the above two registration methods are 0.15 mm and 0.09 mm, respectively. These values have mean absolute errors of 7.7 mm and 2.5 mm and root mean square errors of 9.3 mm and 3.3 mm, respectively. In terms of both MAE and RMSE, the overall registration error of the point cloud data is reduced by 65% for the coordinate-based registration method compared to the point-based registration method. These data indicate that the proposed coordinate-based registration method has a significant improvement in accuracy compared to the point-based registration method at the global registration stage.

In the field of fine registration of point clouds, the ICP algorithm has long been considered the most classical registration algorithm and has been widely used for many years [37, 38]. ICP can be categorized into point-to-point and point-to-plane methods based on the way the error metric is calculated [39]. The point-to-point method uses the distance between corresponding points in two clouds [40]. The point-to-plane method utilizes the distance between a point in the first cloud and a tangent plane in the second cloud [3]. The two sets of global point clouds are finely aligned using the point-to-point and point-to-plane ICP registration algorithms, respectively, and the error statistics of the two sets of point clouds are shown in Table 4. The registration errors for the two sets of global point clouds with different mileage are shown in Figures 12 and 13. Both fine-registration algorithms are effective in improving the overall accuracy of the global point cloud. RMSE of the two global point clouds processed by the point-to-point method is 3.6 mm and 3.1 mm, respectively. Correspondingly, RMSE of the two global point clouds processed by the point-to-plane method is 4.6 mm and 3.2 mm, respectively.

In the test scenes of this paper, the point-to-point ICP algorithm performs better and achieves more accurate registration. The above phenomenon is mainly due to the following factors: (1) point-to-plane ICP algorithms use surface normal and take advantage of the tendency of most point cloud data to be locally planar [41]. However, the secondary lining of the tunnel belongs to a typical circular cross-section, and the assumption that most point cloud data are locally planar is difficult to realize, which reduces the

registration accuracy of the point-to-plane algorithm to some extent. (2) Lower point cloud density in the overlapping regions between neighboring stations reduces the accuracy and reliability of the surface normal vectors, which may cause the algorithm to converge to a local minimum or produce suboptimal registration [42]. The point-to-point method achieves point cloud registration by minimizing the distance between corresponding points, which is more robust and applicable in nonplanar scenes [42]. Overall, the point-to-point ICP algorithm is more suitable for the scene in the paper and achieves higher accuracy for the registration of the two sets of global point clouds.

The fine registration is done in PCL, and the main factors affecting the accuracy of the point-to-point ICP algorithm registration are as follows: the initial registration accuracy, the corresponding point distance threshold, the number of calculated points, and the number of iterations. The two groups of point clouds have been globally registered, with good initial registration accuracy, which can effectively avoid the problem of locally optimal solutions [37]. During the operation of the ICP algorithm, for the extraction of the corresponding points of the reference and target point clouds, the nearest neighbor points of each point of the target point cloud are first searched in the reference point cloud, and then the corresponding point distance threshold is used to judge whether this group of points is a corresponding point or not. The point cloud densities of the data used in this paper are inconsistent, with the highest point density having a point spacing of 7.5 mm and the lowest point density having a point spacing of 5 cm. Since the global registration of the two sets of point clouds has been completed, the corresponding point spacing will be further reduced, and in order to ensure the reliability of the corresponding point extraction, we set the corresponding point distance threshold to half of the minimum value of the point spacing, i.e., 4 mm. The number of calculation points, i.e. the number of points involved in the calculation during the corresponding point search process, affects the calculation efficiency and registration accuracy of the ICP algorithm [42]. Researchers generally select an appropriate number of initial computational point clouds by downsampling methods such as uniform sampling [43], random sampling [44], or feature-based sampling [45]. However, the point density of the point cloud used in this paper is not very high, and downsampling will further reduce the point cloud density, which is not conducive to registration accuracy. Each station cloud has already been orientated to the reference coordinate system, and we use the tunnel mileage information to extract the specified length of the point cloud for the calculation of the translation matrix and rotation moments and then achieve the fine registration of each station cloud. It should be noted that the points involved in the computation are located in the common scanning area of the neighboring stations, as shown in Figure 14. We use the distribution length of the computed point cloud to characterize the volume of the point cloud. The registration effectiveness of the ICP algorithm is generally judged using the root mean square (RMS) absolute value of the corresponding point distances. Due to the inconsistent point cloud density in different regions, this means that larger RMS absolute values may have smaller errors when the density of the point cloud involved in the calculation is low. When the overall density of the point cloud involved in the calculation is high, a smaller absolute value of RMS does not indicate better registration accuracy [37]. For the above reasons, we use the overall error of the fine-registration point cloud to evaluate the registration effect under different conditions of the number of computed points, and the index used for evaluation is MAE. The fine-registration process starts with station #S1 as the reference point cloud, and the remaining stations are used as the target point cloud, in turn, to complete the registration, with 100 iterations for each registration iteration.

MAE for the two sets of data under different computational point conditions is shown in Figure 15. When the distribution length of the computed points is 12–14 m, MAE of both sets of global point clouds is gradually stabilized to 2.7 mm and 2.3 mm, respectively. It is worth noting that when fewer calculation points are selected, due to the lower density of points on both sides of the centreline of the two stations, the number of corresponding points obtained is lower and the reliability is also the lowest, and the final accuracy of the registration is also lower. When the distribution area of the points involved in the calculation gradually increases, the density of the point cloud of the two stations will increase sharply with the decrease in the distance from the laser emission point, and the number and reliability of the corresponding points will also increase significantly, and the effect of fine registration will also be improved. However, as the number of points involved in the calculation increases, the length of the calculation also increases dramatically. Under comprehensive consideration of accuracy and efficiency, we choose the points on both sides of the centreline with a total area of 14 m as the calculation points. Other parameters are shown in Table 5.

In the fine-registration stage, the point-to-point ICP algorithm is used to fine-align the two sets of global point cloud data. After fine registration, the overall offset of the global point clouds obtained by the point-based registration method is significantly reduced, and MAE and RMSE are reduced from the initial 7.7 mm and 9.6 mm to 2.7 mm and 3.6 mm, respectively, with a 65% and 62% reduction in the offset, and the accuracy of the registration is significantly improved. In contrast, the accuracy of the global point cloud obtained by the coordinate-based registration method is not significantly improved, and the MAE and RMSE are reduced by 8% and 6%, respectively. The global point cloud obtained by the coordinate-based registration method has a better accuracy, which is basically up to the level of fine registration, so there is limited room for the ICP algorithm to improve the accuracy of the global point cloud, as shown in Figures 11 and 13. The coordinate-based registration method achieves automatic registration and positioning of the point cloud at each station by precisely locating the coordinates and directions of the scanned points in the reference coordinate system prior to the data acquisition process. Compared with the point-based registration method, the above method effectively avoids the problems of

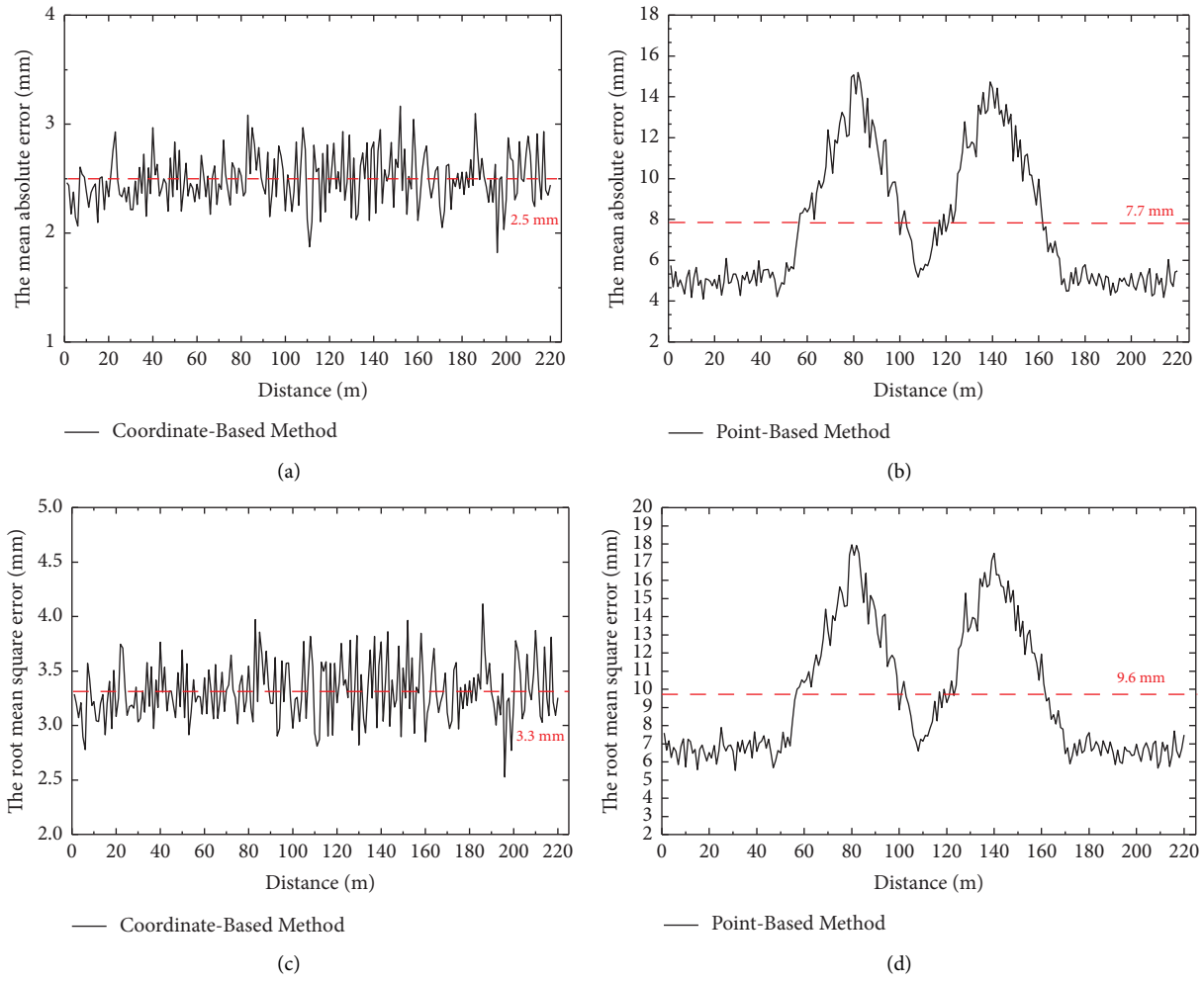

Figure 11: Global registration stage accuracy evaluation index.

Table 4: Error statistics (mm).

Methods	The mean absolute error (MAE)	The root mean square error (RMSE)
Point-based method + point-to-plane	3.5	4.6
Coordinate-based method + point-to-plane	2.4	3.2
Point-based method + point-to-point	2.7	3.6
Coordinate-based method + point-to-point	2.3	3.1

target displacement, and feature point extraction greatly reduces human-introduced errors and accidental errors and significantly improves the accuracy of global registration. The overall registration errors of the two sets of global point clouds at different stages of registration are shown in Table 6.

Furthermore, the coordinate-based registration method effectively reduces the effect of propagation errors. According to Figure 11, the point cloud obtained by the point-based registration method exhibits obvious error propagation. Since #*S*1, #*S*2, and #*S*3 stations are aligned with #*M*1 targets, #*S*3, #*S*4, and #*S*5 stations are aligned with #*M*2 targets. Therefore, when a small amount of error exists in the registration process, the error will gradually accumulate and the offset will gradually increase as the testing distance increases. Due to the arrangement of stations at #*S*3, the point cloud density and accuracy are greatly improved. This finally leads to the peak of the overall point cloud offset at 80 m and 140 m as shown in Figures 11 and 13. The point cloud is finely aligned, and the influence of propagation error is significantly reduced, but it still exists, as shown in Figure 11. In terms of the consistency of the offset error obtained by the coordinate-based registration method, it is significantly better than the point-based registration method, the propagation error is effectively controlled, and the final accuracy and effectiveness of the point cloud are significantly improved. Moreover, coordinate-

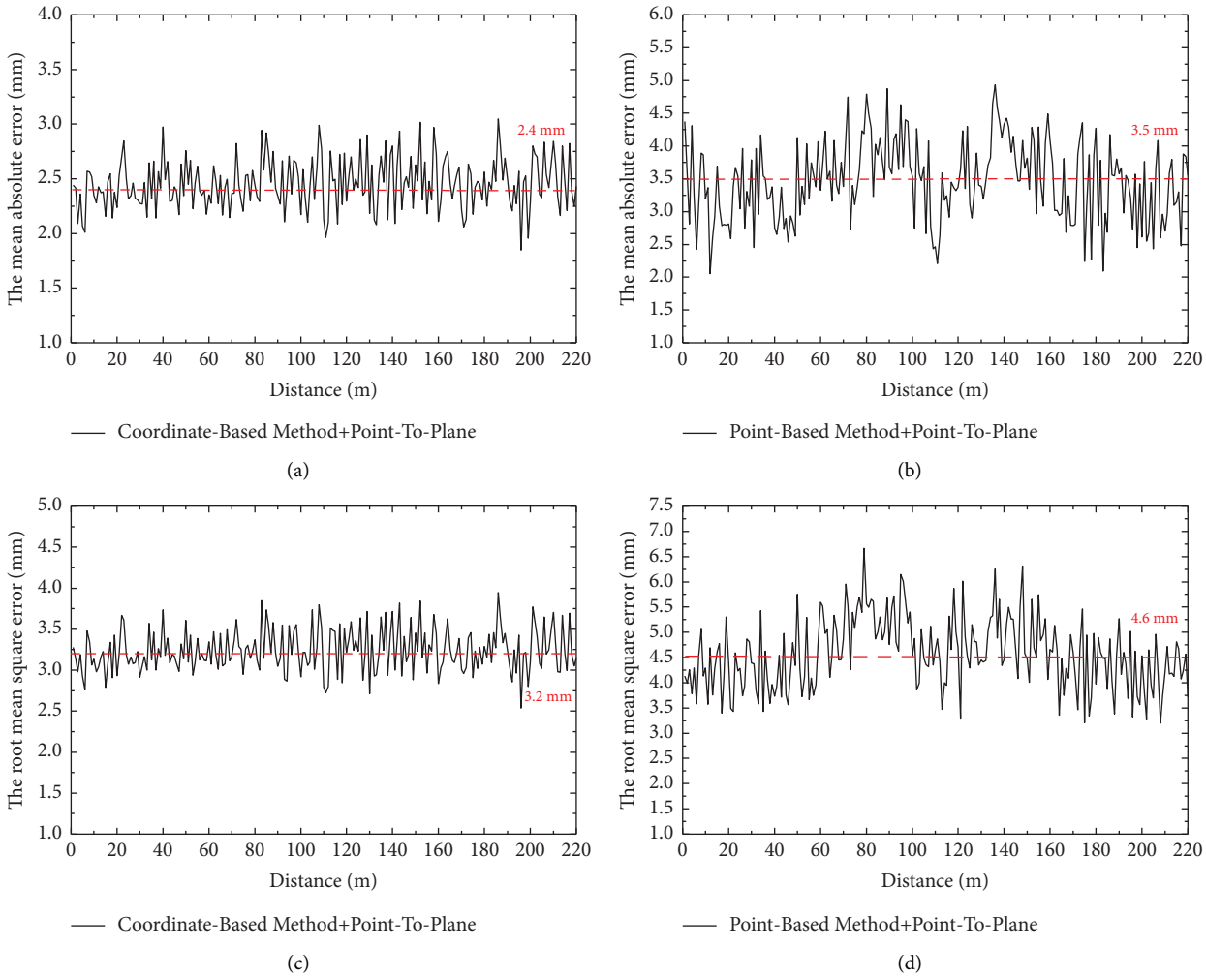

Figure 12: Point-to-plane ICP registration accuracy evaluation index.

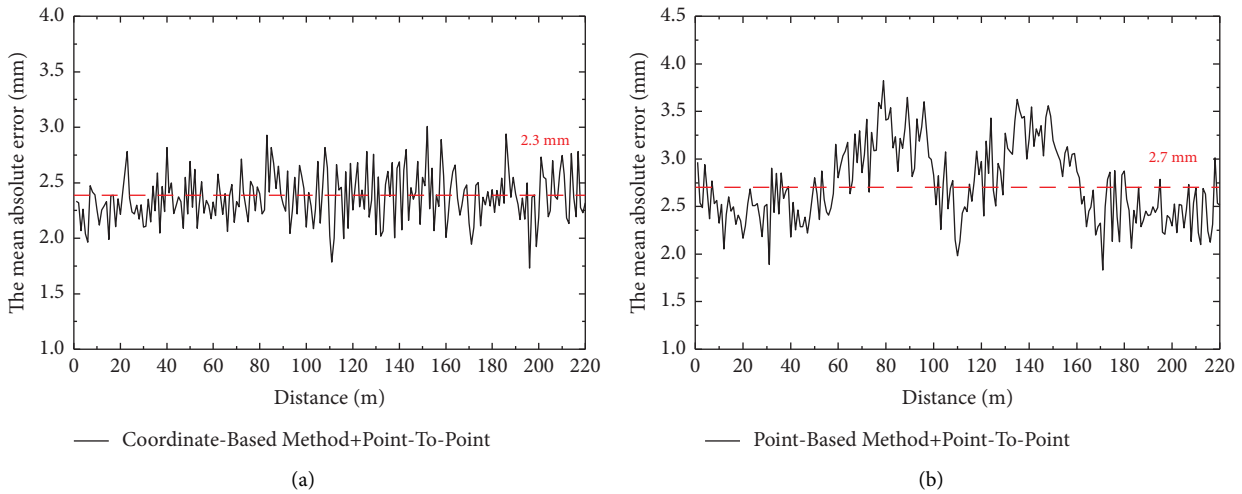

Figure 13: Continued.

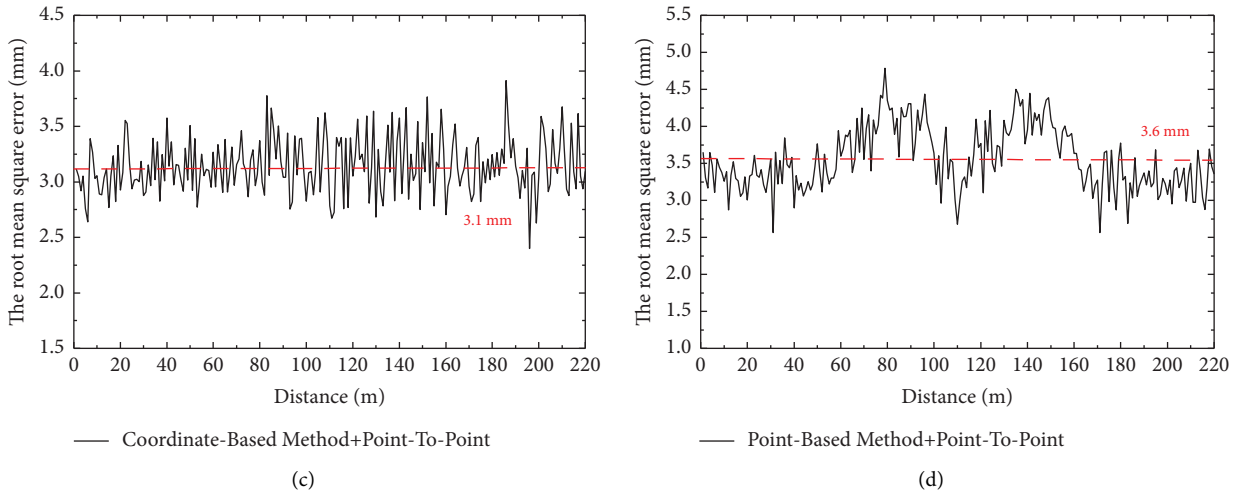

Figure 13: Point-to-point ICP registration accuracy evaluation index.

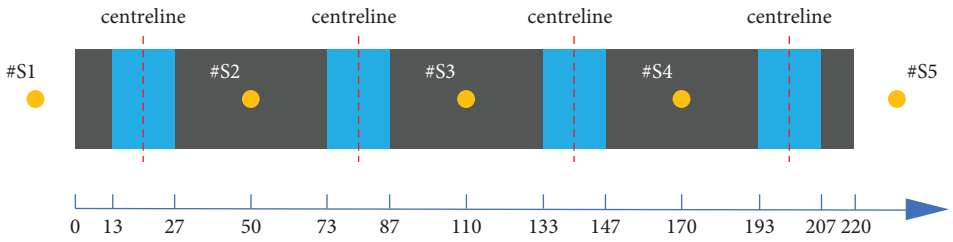

Figure 14: Schematic of the distribution of calculation points.

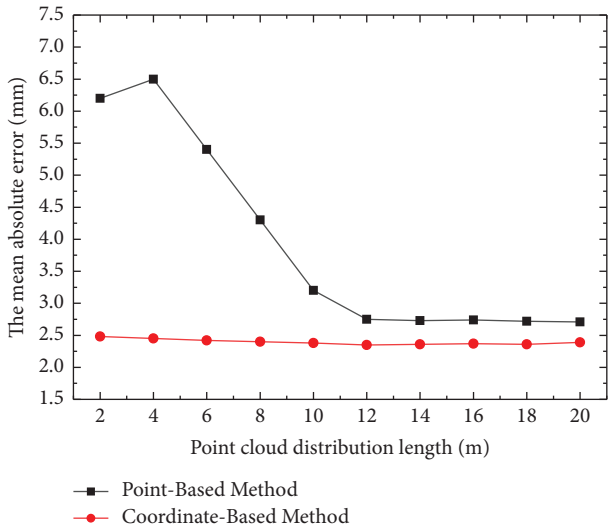

Figure 15: Effect of point distribution length on registration accuracy.

based registration relies on the accurate positioning of the scanning point coordinates and the orientation of the reference coordinate system, and its error sources are primarily caused by systematic errors of the acquisition equipment and the construction errors of the actual tunnel structure. In general, the coordinate-based registration method is significantly better than the most widely used point-based registration method in terms of registration accuracy, and the registration error is reduced by 65%, which has reached the fine-registration level. In this paper, a refined inverse reconstruction of the tunnel structure has been achieved, which also shows that the global point cloud of the tunnel

Table 5: Point-to-point ICP algorithm parameters.

Parameters	Point-based method	Coordinate-based method
Initial registration accuracy (MAE)	7.7 mm	2.5 mm
Distance threshold	4 mm	4 mm
Point distribution length	14 m	14 m
Number of iterations	60	60
Fine-registration accuracy (MAE)	2.7 mm	2.3 mm

structure obtained by the coordinate-based registration method has high accuracy and can well meet the accuracy needs of the monitoring and measurement work of the tunnel structure throughout its life cycle.

In terms of efficiency, the feature point-based registration method includes data acquisition, feature point extraction, and registration calculation, and the total time spent in this experiment is 200 minutes. The coordinate-based registration method completes the data positioning and registration at the data acquisition stage, and the global registration of each station cloud is completed by importing the data into the TBC, which takes 150 minutes in total, and the efficiency is improved by 25%. The coordinate-based registration method can avoid the process of feature point extraction, registration calculation, and positioning adjustment in the global registration process and is significantly better than the point-based registration method in terms of registration efficiency and automation. In comparison with the widely used global registration method, coordinate-based registration has 25% higher efficiency and 65% lower registration error, reaching the level of fine registration required for fine inverse modeling of tunnel structures.

4.5. Validation Experiments. In order to verify the registration accuracy, applicability, and robustness of the coordinate-based global registration method in complex scenes, in this part, we selected a curved railway tunnel for repeated measurements and further analyzed the influence of the control point positioning accuracy on the positioning accuracy of the scanning point and the registration accuracy.

4.5.1. Verification of Global Registration Accuracy for Curved Railway Tunnel. We selected a curve railway tunnel with a design length of 2000 m as the test object, the measurement section has completed the construction of the second lining, the length is 300 m, the curve radius is 7.5 km, and the slope is 1.2%. We set up six stations with a spacing of 60 m and a standard sampling pattern to ensure that there are at least six points in each square decimeter and used a coordinate-based registration method to align the point cloud of the six stations. The global point cloud is shown in Figure 16. The global point cloud can effectively present the geometric information of the secondary lining as a whole at the macrolevel. At the fine level, the global point cloud can still effectively present the detailed features of the tunnel with high recognizability, as shown in Figure 17.

In order to effectively verify the registration accuracy of the global point cloud for curved railway tunnels, we designed the following experiments. We configured corresponding auxiliary feature points for each of the six stations and measured the accurate coordinates of the auxiliary feature points under the reference coordinate system using a total station. Subsequently, we extracted the coordinate information of the corresponding feature points from the global point cloud and compared the coordinate information of the auxiliary feature points obtained by the two measurement methods, so as to verify the registration accuracy of the coordinate-based registration method under curve conditions. It is worth noting that due to the very high uniformity of the tunnel cross-section, there is a lack of distinctive feature points and structures, as shown in Figure 17. If a total station is used to measure a specific point on the tunnel surface, we cannot accurately identify and extract the corresponding measurement point in the global point cloud. Based on the above reasons, we place a rectangular target in the effective scanning area of each station, select the two corners of the upper part of the target as the feature points, and set up the targets and stations as shown in Figure 18. We did not use spherical targets or prisms to construct auxiliary feature points, because it was not possible to accurately measure the spherical center coordinates of the target ball for the total station, and the 3D laser scanner was not able to capture the point cloud inside the prism.

We take the measurement results of the total station as the reference coordinates, and the difference between the coordinates of the feature points under the global point cloud and the reference coordinates is the positioning and registration error of each station under the reference coordinate system. The error statistics of the 12 auxiliary feature points are shown in Table 7, and the average error is 0.8 mm, the RMSE is 0.9 mm, and the absolute median error is 0.8 mm. The above tests show that the coordinate-based registration method still has high applicability and robustness under curved conditions and is able to realize the accurate positioning and registration of the multi-station clouds in curved railway tunnels with high accuracy. It should be noted that, in part 4.4, for the accuracy verification of the global point cloud of the linear tunnel, we compare the global point cloud with the designed cross-section and then calculate the overall registration accuracy of the global point cloud. However, in the actual project, construction error is inevitable, and there is a difference between the reference cross-section and the actual cross-section, so the RMSE obtained is larger. For the global registration accuracy verification of curved railway tunnels, we use the difference between the measured values of the coordinates of the feature points and the reference value as

Table 6: Error statistics (mm).

Step	Methods	The average of the algebraic deviations	The mean absolute error (MAE)	The root mean square error (RMSE)
Global registration	Point-based method	0.15	7.7	9.6
	Coordinate-based method	0.09	2.5	3.3
	Point-based method + ICP	0.09	2.7	3.6
	Coordinate-based method + ICP	0.084	2.3	3.1

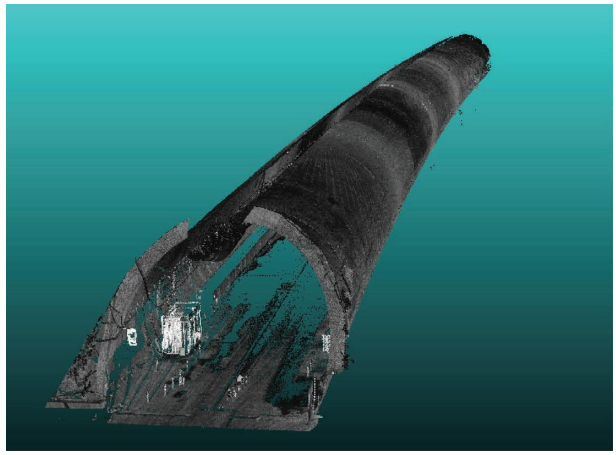

Figure 16: Global point cloud of the curved tunnel.

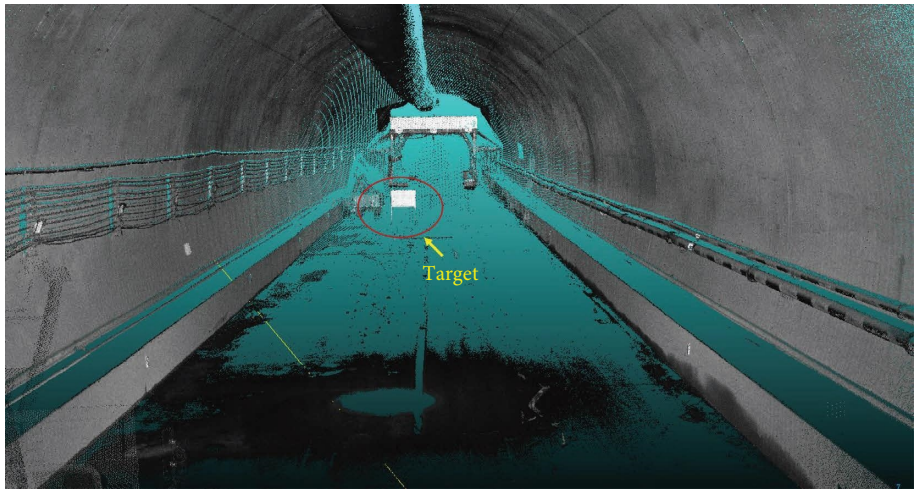

Figure 17: Detailed point cloud of the curved railway tunnel.

the evaluation index of the registration accuracy. Because the reference value is more accurate, RMSE obtained is smaller.

4.5.2. Effect of Control Point Accuracy on Registration Accuracy. The coordinate-based global registration method uses the control points to realize the positioning of the coordinates and directions of the laser scanning points in the reference coordinate system, then realizes the positioning of each station cloud independently to the reference coordinate system during the data collecting process, and ultimately realizes the automated and accurate registration of multiple station clouds. In the above process, the control point accuracy and laser scanner leveling accuracy directly affect the positioning accuracy of the laser scanning points and global registration accuracy. Currently, mainstream 3D laser scanners are equipped with mechanical or electronic compensators, so we can easily and accurately level the scanner. The leveling accuracy of the scanner can be effectively controlled and will not limit the practical application of the coordinate-based registration method. In this part, we quantitatively analyze the effect of control point accuracy on laser scanning point positioning accuracy and global registration accuracy through experiments.

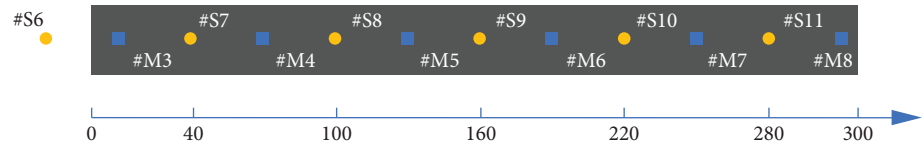

Figure 18: Schematic diagram of measuring station and target setting.

Table 7: Error statistics (mm).

Indicators	Mean error	Root mean square error	Median absolute error
Value	0.8	0.9	0.8

The setting of measuring stations and auxiliary feature points in the test part is consistent with part 4.5.1. There are two ways to introduce errors: (1) the control point position is moved, and the control point coordinate information is constant. (2) The control point position is constant, and the control point coordinate information is changed. However, applying exact displacement to the control point is difficult, and we change the control point coordinate information, which in turn adds error to the control point.

The test procedure is as follows: first, the laser emission point is localized using the method in part 3.1 to obtain its coordinates under the reference coordinate system. Then, the error is quantitatively introduced to one control point, and the coordinates of the other control point are constant. Finally, the difference between the coordinates of the laser scanning point and the true coordinates is calculated. The value range of the error is 0–25 mm, and the introduction of the error is gradually increased in steps of 1 mm, and the error is introduced in the way as shown in the following equation:

$$\begin{bmatrix} X \\ Y \\ Z \end{bmatrix} = \begin{bmatrix} x \\ y \\ z \end{bmatrix} + k \begin{bmatrix} m \\ u \\ v \end{bmatrix}, \tag{16}$$

where $(x, y, z)^T$ is the true coordinates of the control point, $(m, u, v)^T$ is a random three-dimensional unit vector, k is the error, and $(X, Y, Z)^T$ is the corrected control point coordinates.

It should be noted that we use the total station to verify the accuracy of the control points, and the relative error of the two control points under the reference coordinate system is 0.3 mm, and we take the initial coordinates of the control points as the reference.

Under different accuracy conditions, the positioning error of the laser scanning point is shown in Figure 19(a). Through the observation of Figure 19(b), it is easy to find that with the gradual decrease of the accuracy of the control point, the positioning accuracy of the laser scanning point is also gradually reduced, and the two are linearly correlated. As a whole, the error values of the control points are roughly the same as the positioning error values of the laser scanning points, as shown by the blue reference line in Figure 19.

The core of the coordinate-based global registration method is positioning, which positions each station cloud independently to a reference coordinate system, thus realizing automated registration of the global point cloud. Since the positioning process of each station cloud does not affect each other, there is no propagation error, and the positioning accuracy of each station cloud is the registration accuracy of the scanned area. The impact of control point accuracy on the positioning precision of individual station clouds is equivalent to its effect on the accuracy of global point cloud registration.

We set up the following experiment to study the effect of control point accuracy on the point cloud registration accuracy. First, we used a total station to accurately measure the true coordinates of the feature points of the #M3, #M4, and #M5 targets in a reference coordinate system, set as the reference coordinates, with the feature points numbered #M3-1, #M3-2, #M4-1, #M4-2, #M5-1, and #M5-2, respectively. Subsequently, errors are gradually introduced to the control points, and the rotation and translation matrices corresponding to each station with different error levels are calculated to complete the localization and orientation calibration of the laser scanning points of each station. Then, the point cloud data acquisition and global registration of the three stations are completed, and the coordinate information of the feature points is extracted from the global point cloud. Finally, the measured coordinates of the feature points are compared with the reference coordinates to calculate the positioning and registration accuracy of each station cloud.

In the above experiment, we set the error step to 1 mm, and the error range is 0–25 mm. The positioning errors of the feature points of each station under different error levels are shown in Figure 16(b). The positioning errors of the feature points at the same station are basically the same, so for each station, we selected only one feature point to show the error variation. The effect of control point accuracy on the positioning and registration accuracy of a specific measurement point is also linear, which is consistent with the laser scanning point; as the control point error gradually increases, the positioning error of the feature point also gradually increases. However, the effect of control point accuracy on specific measurement point accuracy is somewhat more pronounced. Overall, for every 1 mm

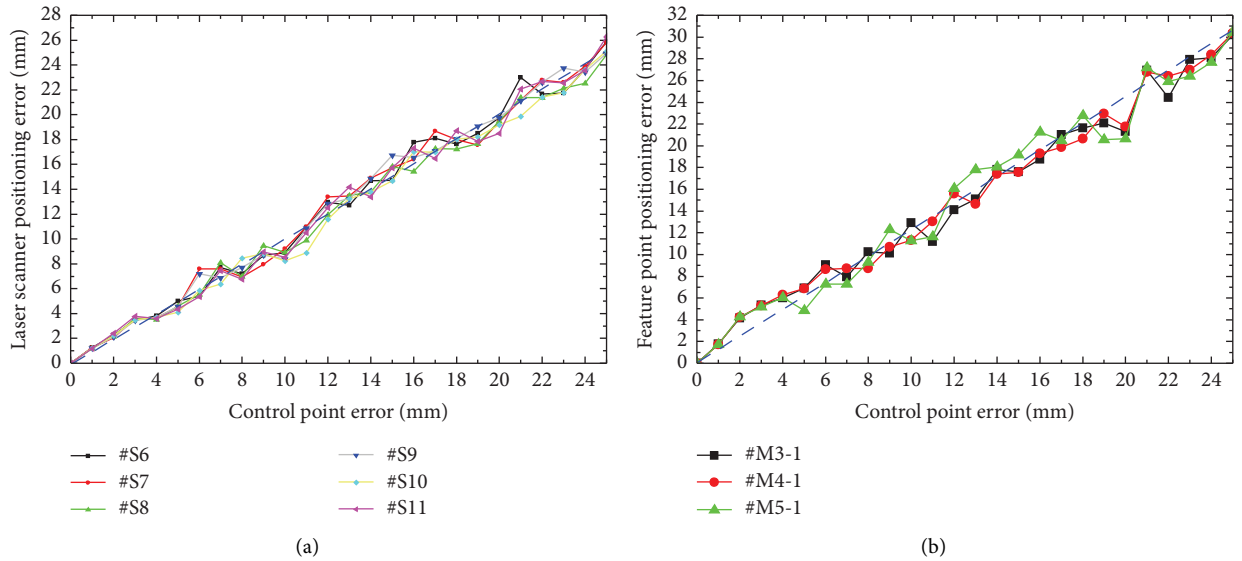

Figure 19: (a) Influence of control point accuracy on the positioning accuracy of laser scanning points and (b) influence of control point accuracy on the positioning and registration accuracy of measuring points.

increase in control point error, the positioning error of the measurement point will increase by 1.2 mm, while the increase in positioning error of the scanning point is 1 mm, as shown by the blue reference line in Figure 19. For the positioning of the laser scanning point, only one measurement is needed, while the measurement of the feature point and the specific point needs to be measured twice, and there is an error accumulation problem in this process, so the control point accuracy has a more obvious impact on the positioning and registration accuracy of the point cloud.

Overall, when the control point accuracy is at the millimeter level, the coordinate-based registration method is still able to achieve millimeter-level positioning and global registration.

For railway tunnel engineering, the control point error of the CPIII network is less than 1 mm, and this accuracy is fully satisfied with the positioning and registration needs. Also, the construction personnel will regularly check and correct each control point, which effectively ensures the quality of the control points of the CPIII network, and the coordinate-based registration method has good applicability in the field of railway tunnel engineering. However, not all measurement environments can provide high-quality control points. Missing control points and displacement and accuracy variations, as well as error correction are all issues that we need to consider, and these issues are the focus of our future research work.

5. Conclusions

TLS technology has obvious advantages over traditional monitoring and measurement methods given its wide detection range, high sampling efficiency, and low time costs. It is, therefore, a common tool for engineering measurements of infrastructure. However, the application of TLS technology in the field of railway tunnels faces many obstacles. Point-based global registration is difficult to achieve high registration accuracy due to the lack of obvious feature structure and the linear distribution of railway tunnels, and it is easy to create propagation errors during the process of global registration of multistation clouds, which negatively impacts the accuracy of the global point cloud and the validity of detection results. For the registration and positioning of 3D point clouds of railway tunnels, a coordinate-based precise positioning and registration method is presented in this paper. This method uses a small number of control points to locate the scanned points of each station and to determine the direction of the reference coordinate system. This method aims at accurate positioning and automatic registration of the cloud of each station in the reference coordinate system during data acquisition. In the coordinate-based registration method, each station cloud is aligned to the reference coordinate system independently, rather than sequentially. This prevents the initial registration error of each station cloud from having a cumulative effect and causing a propagation error. As a result, the coordinate-based registration method eliminates the introduction of error through artificial target setting and feature point extraction, as well as solving the problem of accurate positioning of a point cloud within the reference coordinate system, which significantly improves the accuracy, efficiency, and automation of multistation clouds registration. The experiment demonstrates that the coordinate-based global registration method is still robust and applicable in complex scenes, and it is suitable for the accurate positioning and registration of multistation clouds in linear and curved railway tunnels. In contrast with the most commonly used point-based global registration method in the field of railway tunnels, the coordinate-based registration method has a 25% improvement in efficiency and a 65% reduction in registration error. Global point cloud registration has reached the level of fineness required for fine-grained inverse modeling of railway tunnels.

Data Availability

The data presented in this study are available on request from the corresponding author. The data are not publicly available due to project requirements.

Conflicts of Interest

The authors declare that there are no conflicts of interest.

Acknowledgments

The authors would like to thank Professor Shi Qiu of Central South University for his support of this study. This work was supported by the National Natural Science Foundation of China (Nos. U1734208 and 52178442).

References

[1] D. Jia, W. Zhang, and Y. Liu, "Systematic approach for tunnel deformation monitoring with terrestrial laser scanning," *Remote Sensing*, vol. 13, no. 17, p. 3519, 2021.

[2] V. Gikas, "Three-dimensional laser scanning for geometry documentation and construction management of highway tunnels during excavation," *Sensors*, vol. 12, no. 8, pp. 11249–11270, 2012.

[3] T. Nuttens, C. Stal, H. De Backer, K. Schotte, P. Van Bogaert, and A. De Wulf, "Methodology for the ovalization monitoring of newly built circular train tunnels based on laser scanning: liefkenshoek Rail Link (Belgium)," *Automation in Construction*, vol. 43, pp. 1–9, 2014.

[4] Q. Jiang, S. Zhong, P. Z. Pan, Y. Shi, H. Guo, and Y. Kou, "Observe the temporal evolution of deep tunnel's 3D deformation by 3D laser scanning in the Jinchuan No. 2 mine," *Tunnelling and Underground Space Technology*, vol. 97, Article ID 103237, 2020.

[5] J. Y. Han, J. Guo, and Y. S. Jiang, "Monitoring tunnel deformations by means of multi-epoch dispersed 3D LiDAR point clouds: an improved approach," *Tunnelling and Underground Space Technology*, vol. 38, pp. 385–389, 2013.

[6] C. Yi, D. Lu, Q. Xie et al., "Hierarchical tunnel modeling from 3D raw LiDAR point cloud," *Computer-Aided Design*, vol. 114, pp. 143–154, 2019.

[7] W. Mukupa, G. W. Roberts, C. M. Hancock, and K. Al-Manasir, "A review of the use of terrestrial laser scanning application for change detection and deformation monitoring of structures," *Survey Review*, vol. 49, no. 353, pp. 1–18, 2016.

[8] M. Pejić, "Design and optimisation of laser scanning for tunnels geometry inspection," *Tunnelling and Underground Space Technology*, vol. 37, pp. 199–206, 2013.

[9] Y. Reshetyuk, *Self-calibration and direct georeferencing in terrestrial laser scanning*, KTH, Stockholm, Sweden, PhD, 2009.

[10] M. Zheng, Y. Zhang, J. Zhu, and X. Xiong, "Self-calibration adjustment of CBERS-02B long-strip imagery," *IEEE Transactions on Geoscience and Remote Sensing*, vol. 53, no. 7, pp. 3847–3854, 2015.

[11] L. Cheng, S. Chen, X. Liu et al., "Registration of laser scanning point clouds: a review," *Sensors*, vol. 18, no. 5, p. 1641, 2018.

[12] T. Urbančič, Ž. Roškar, M. Kosmatin Fras, and D. Grigillo, "New target for accurate terrestrial laser scanning and unmanned aerial vehicle point cloud registration," *Sensors*, vol. 19, no. 14, p. 3179, 2019.

[13] M. Weinmann, *Reconstruction and Analysis of 3D Scenes: From Irregularly Distributed 3D Points to Object Classes*, Springer, Singapore, 2016.

[14] R. B. Rusu, N. Blodow, and M. Beetz, "Fast point feature histograms (FPFH) for 3D registration," in *Proceedings of the IEEE International Conference on Robotics and Automation*, Kobe, Japan, May 2009.

[15] A. E. Johnson and M. Hebert, "Using spin images for efficient object recognition in cluttered 3D scenes," *IEEE Transactions on Pattern Analysis and Machine Intelligence*, vol. 21, no. 5, pp. 433–449, 1999.

[16] S. Barnea and S. Filin, "Registration of terrestrial laser scans via image based features," in *Proceedings of the ISPRS Commission V Symposium 'Image Engineering and Vision Metrology*, Dresden, Germany, March 2007.

[17] Z. Kang, J. Li, L. Zhang, Q. Zhao, and S. Zlatanova, "Automatic registration of terrestrial laser scanning point clouds using panoramic reflectance images," *Sensors*, vol. 9, no. 4, pp. 2621–2646, 2009.

[18] R. Sensing and L. Road, "Point based registration of terrestrial laser data using intensity and geometry features," *IAPRS and SIS*, vol. 37, pp. 583–590, 2008.

[19] R. Hänsch, T. Weber, and O. Hellwich, "Comparison of 3D interest point detectors and descriptors for point cloud fusion," *ISPRS Annals of the Photogrammetry, Remote Sensing and Spatial Information Sciences*, vol. 2, pp. 57–64, 2014.

[20] A. Gressin, C. Mallet, J. Ô. Demantké, and N. David, "Towards 3D lidar point cloud registration improvement using optimal neighborhood knowledge," *ISPRS Journal of Photogrammetry and Remote Sensing*, vol. 79, pp. 240–251, 2013.

[21] D. Aiger, N. J. Mitra, and D. Cohen-Or, "4-Points congruent sets for robust pairwise surface registration," *ACM Transactions on Graphics*, vol. 27, no. 3, pp. 1–10, 2008.

[22] J. Sun, R. Zhang, S. Du, L. Zhang, and Y. Liu, "Global adaptive 4-Points congruent sets registration for 3d indoor scenes with robust estimation," *IEEE Access*, vol. 8, pp. 7539–7548, 2020.

[23] W. V. Hansen, H. Gross, and U. Thoennessen, "Line-based registration of terrestrial and airborne lidar data," *The International Archives of the Photogrammetry, Remote Sensing and Spatial Information Sciences*, vol. 37, pp. 161–166, 2008.

[24] B. Yang, Y. Zang, Z. Dong, and R. Huang, "An automated method to register airborne and terrestrial laser scanning point clouds," *ISPRS Journal of Photogrammetry and Remote Sensing*, vol. 109, pp. 62–76, 2015.

[25] J. Lee, K. Yu, Y. Kim, and A. F. Habib, "Adjustment of discrepancies between LIDAR data strips using linear features," *IEEE Geoscience and Remote Sensing Letters*, vol. 4, no. 3, pp. 475–479, 2007.

[26] A. Habib, M. Ghanma, M. Morgan, and R. Al-Ruzouq, "Photogrammetric and lidar data registration using linear features," *Photogrammetric Engineering & Remote Sensing*, vol. 71, no. 6, pp. 699–707, 2005.

[27] K. Al-Durgham and A. Habib, "Association-matrix-based sample consensus approach for automated registration of terrestrial laser scans using linear features," *Photogrammetric Engineering & Remote Sensing*, vol. 80, no. 11, pp. 1029–1039, 2014.

[28] O. Monserrat and M. Crosetto, "Deformation measurement using terrestrial laser scanning data and least squares 3D surface matching," *ISPRS Journal of Photogrammetry and Remote Sensing*, vol. 63, no. 1, pp. 142–154, 2008.

[29] C. Dold and C. Brenner, "Automatic matching of terrestrial scan data as a basis for the generation of detailed 3D city

models," *International Archives of Photogrammetry and Remote Sensing*, vol. 35, 1996.

[30] C. Brenner, C. Dold, and N. Ripperda, "Coarse orientation of terrestrial laser scans in urban environments," *ISPRS Journal of Photogrammetry and Remote Sensing*, vol. 63, no. 1, pp. 4–18, 2008.

[31] Y. J. Cheng, W. G. Qiu, and D. Y. Duan, "Automatic creation of as-is building information model from single-track railway tunnel point clouds," *Automation in Construction*, vol. 106, Article ID 102911, 2019.

[32] L. Tao, T. Nguye, T. Nguyen, T. Ito, and T. Bui, "An adaptive differential evolution algorithm with a point-based approach for 3D point cloud registration," *Journal of Image and Graphics*, vol. 10, no. 1, 2022.

[33] Z. Zhang, L. Sun, R. Zhong et al., "3-D deep feature construction for mobile laser scanning point cloud registration," *IEEE Geoscience and Remote Sensing Letters*, vol. 16, no. 12, pp. 1904–1908, 2019.

[34] K. Chaiyasarn, T. K. Kim, F. Viola, R. Cipolla, and K. Soga, "Distortion-free image mosaicing for tunnel inspection based on robust cylindrical surface estimation through structure from motion," *Journal of Computing in Civil Engineering*, vol. 30, no. 3, 2016.

[35] D. Hu, Y. Li, X. Yang, X. Liang, K. Zhang, and X. Liang, "Experiment and application of NATM tunnel deformation monitoring based on 3D laser scanning," *Structural Control and Health Monitoring*, vol. 2023, Article ID 3341788, 13 pages, 2023.

[36] D. Y. Duan, W. G. Qiu, Y. J. Cheng, Y. C. Zheng, and F. Lu, "Reconstruction of shield tunnel lining using point cloud," *Automation in Construction*, vol. 130, Article ID 103860, 2021.

[37] P. Li, R. Wang, Y. Wang, and W. Tao, "Evaluation of the ICP algorithm in 3D point cloud registration," *IEEE Access*, vol. 8, pp. 68030–68048, 2020.

[38] P. J. Besl and N. D. McKay, "A method for registration of 3-D shapes," *IEEE Transactions on Pattern Analysis and Machine Intelligence*, vol. 14, no. 2, pp. 239–256, 1992.

[39] N. J. Mitra, N. Gelfand, H. Pottmann, and L. Guibas, "Registration of point cloud data from a geometric optimization perspective," *Proceedings of the 2004 Eurographics/ACM SIGGRAPH symposium on Geometry processing*, vol. 71, 2004.

[40] G. Champleboux, S. Lavallee, R. Szeliski, and L. Brunie, "From accurate range imaging sensor calibration to accurate model-based 3D object localization," in *Proceedings of the IEEE Computer Society Conference on Computer Vision and Pattern Recognition*, Champaign, IL, USA, June 1992.

[41] W. Liu, H. Wu, and G. S. Chirikjian, "LSG-CPD: coherent point drift with local surface geometry for point cloud registration," in *Proceedings of the 2021 IEEE/CVF International Conference on Computer Vision (ICCV)*, Montreal, Canada, October 2022.

[42] Y. He, B. Liang, J. Yang, S. Li, and J. He, "An iterative closest points algorithm for registration of 3D laser scanner point clouds with geometric features," *Sensors*, vol. 17, no. 8, p. 1862, 2017.

[43] G. Turk and M. Levoy, "Zippered polygon meshes from Range images," in *Proceedings of the 21st Annual Conference on Computer Graphics and Interactive Techniques*, Orlando, FL, USA, July 1994.

[44] T. Masuda, K. Sakaue, and N. Yokoya, "Registration and integration of multiple range images for 3-D model construction," in *Proceedings of 13th International Conference on Pattern Recognition*, Vienna, Austria, August 1996.

[45] A. D. Sappa, A. Restrepo-specht, and M. Devy, "Range image registration by using an edge–based representation," in *Proceedings of th 9th International Symposium on Intelligent Robotic Systems SIRS*, Toulouse, France, July 2001.